Available online at www.sciencedirect.com
SCIENCE DIRECT
Cement and Concrete Research 36 (2006) 18 – 29
Cement and Concrete Research

The role of Al in C–S–H: NMR, XRD, and compositional results for precipitated samples☆

G.K. Sun[a], J. Francis Young[a,b], R. James Kirkpatrick[a,c,*]

[a]Center for Advanced Cement-Based Materials, University of Illinois at Urbana-Champaign, Urbana, IL 61801, USA
[b]Departments of Civil and Environmental Engineering and Materials Science and Engineering, University of Illinois at Urbana-Champaign, Urbana, IL 61801, USA
[c]Department of Geology, University of Illinois at Urbana-Champaign, Urbana, IL 61801, USA

Received 23 December 2004; accepted 25 March 2005

Abstract

X-ray diffraction, compositional analysis, and ^{29}Si and ^{27}Al MAS NMR spectroscopy of Al-substituted tobermorite-type C–S–H made by precipitation from solution provide significant new insight into the structural mechanisms of Al-substitution in this important and complicated phase. Al occurs in 4-, 5-, and 6-coordination (Al[4], Al[5], and Al[6]) and plays multiple structural roles. Al[4] occurs on the bridging tetrahedra of the drierkette Al–silicate chains, and Al[5] and Al[6] occur in the interlayer and perhaps on particle surfaces. Al does not enter either the central Ca–O sheet or the pairing tetrahedra of the tobermorite-type layers. Al[4] occurs on three types of bridging sites, Q^3 sites that bridge across the interlayer; Q^2 sites that are charge balanced by interlayer Ca^{+2}, Na^+, or H^+; and Q^2 sites that are most likely charge balanced by interlayer or surface Al[5] and Al[6] through Al[4]–O–Al[5,6] linkages. Although the data presented here are for relatively well-crystallized tobermorite-type C–S–H with C/S ratios $\leq$ 1.2, comparable spectral features for hydrated white cement pastes in previously published papers [30–32] [M.D. Andersen, H.J. Jakobsen, J. Skibsted, Incorporation of aluminum in the calcium silicate hydrate (C–S–H) of hydrated Portland cements: a high-field ^{27}Al and ^{29}Si MAS NMR investigation Inorg. Chem. 42 (2003) 2280–2287; M.D. Andersen, H.J. Jakobsen, J. Skibsted, Characterization of white Portland cement hydration and the C–S–H structure in the presence of sodium aliminate by ^{27}Al and ^{29}Si MAS NMR spectroscopy, Cem. Concr. Res. 43 (2004) 857–868.; M.D. Andersen, H. J. Jakobsen, J. Skibsted, A new aluminum-hydrate phase in hydrated Portland cements characterized by ^{27}Al and ^{29}Si MAS NMR spectroscopy, Cem. Concr. Res., submitted for publication.] indicate the presence of similar structural environments in the C–S–H of such pastes, and by implication OPC pastes.

Keywords: Calcium–silicate–hydrate (C–S–H); Characterization; Crystal structure; Spectroscopy; X-ray diffraction; Alkalis; Aluminum

1. Introduction

Aluminum readily enters the calcium silicate hydrate phase (C–S–H) of Portland cement, and this substitution is expected to play a significant role in many aspects of the chemical behavior of cement paste, including the cation and anion exchange behavior, solubility, and the progress of the reactions that occur during delayed ettringite formation. The C–S–H of slag- and fly ash-based cements is often high in Al, and this can have a significant effect on its suitability in, for instance, hazardous waste applications [1–6]. Despite considerable study, the structural mechanisms of this substitution and its effect on the chemical behavior of cement systems remain a topic of considerable discussion (see Refs. [7–9] for reviews of the C–S–H structure). Kalousek [10] first demonstrated that Al enters the structure of tobermorite (the structural model for many C–S–H samples), suggested that it occurs primarily in the tetrahedral sites substituting for Si, and discussed possible solid solution mechanisms. Copeland et al. [11] demonstrated that the

☆ This research was supported by the NSF Science and Technology Center for Advanced Cement-Based Materials.
* Corresponding author. Center for Advanced Cement-Based Materials, University of Illinois at Urbana-Champaign, Urbana, IL 61801, USA.
E-mail address: kirkpat@uiuc.edu (R..J. Kirkpatrick).

0008-8846/$ - see front matter © 2005 Elsevier Ltd. All rights reserved.
doi:10.1016/j.cemconres.2005.03.002

aluminous phases of hydrated Portland cement, ettringite (AFt), and the hexagonal hydrates (AFm phases), do not account for all of the Al in the cement paste. They also showed that grinding C–S–H with AFm results in disappearance of the AFm and apparent entry on the Al into the C–S–H. More recently, spectroscopic studies have greatly advanced understanding of the role of Al in C–S–H and its model compounds, tobermorite, and jennite [12–33]. There have also been extensive structural studies of the behavior of Al in solutions, aluminate cements, Al-free C–S–H, tobermorite, jennite, and other relevant model materials that help interpret the data for aluminous C–S–H [34–54].

For tobermorite, Komarneni and co-workers [12–15] demonstrated that Al enters primarily tetrahedral coordination (Al[4]), occurs in both Q^2 chain sites and Q^3 sites that link across interlayers, and significantly affects its cation exchange properties. These results and structural interpretations will be key to interpreting the data presented here. Stade and Müller [16] showed that Al occurs as both Al[4] and Al[6] synthetic C–S–H and that the Al[6]/Al[4] ratio increases with increasing Ca/(Si+Al). Kirkpatrick and Cong [17] showed that both Al[4] and Al[6] occur in the C–S–H of hydrated white and ordinary cement pastes, and Skibsted et al. [18,19] showed that Al in both ettringite and AFm phases can be resolved in such pastes. Lognot et al. [20] confirmed that both Al[4] and Al[6] occur in precipitated C–S–H and suggested a structural model that includes Al[6] in the interlayer and Al[4] in both the bridging and pairing tetrahedra of the chains. They also proposed that Na plays an important role in charge balancing the Al[4] for Si[4] substitution.

Faucon et al. [21–25] used MAS and multiple quantum (MQ) ^{27}Al NMR to provide more detailed information about the number and spectroscopic characteristics (isotropic chemical shifts and quadrupolar frequencies) of Al in precipitated, tobermorite-like C–S–H. They resolve two Al[4] sites, one Al[5] site and one Al[6] site that they assign to C–S–H. Their structural model involves Al[4] on both the pairing and bridging tetrahedra of the drierkette tetrahedral chains, Al[5] in the interlayer, and Al[6] substituting for Ca in the central Ca–O sheet. They propose that Al[4] is charge balanced predominantly by H^+(Al–OH groups) and interlayer Na^+, that its abundance decreases with increasing Ca/(Si+Al[4]) ratio, and that it does not occur in tetrahedral dimers that are the dominant tetrahedral sites at high Ca/Si ratios. Schneider et al. [4] confirmed the presence of two Al[4] sites in C–S–H from slag cements, but did not assign the observed Al[6] to the C–S–H phase. Richardson and co-workers [1,2,26–29] used ^{27}Al and ^{29}Si NMR and trimethylsilylation (TMS) to confirm that Al occurs as both Al[4] and Al[6] in C–S–H of slag-containing cement pastes. In their data, the absence of Q^1 sites with 1 Al[4] next-nearest neighbor (Q^1(1Al)), the relative intensities of the ^{29}Si NMR resonances for different sites, and the relative abundances of the silicate polymers of different lengths observed in the TMS data are all consistent with Al[4] occupying only the bridging tetrahedral sites of the drierkette chains. Based on Al-EELS, Brydson et al. [28] and Richardson et al. [1] proposed that Al in the outer-product C–S–H of a slag cement occurs primarily as Al[4] but that in the inner product it occurs as both Al[4] in C–S–H and as Al[6] in a Mg,Al-rich phase similar to hydrotalcite.

More recently, Andersen and co-workers [30–32] have used ^{29}Si NMR, ^{27}Al NMR at multiple fields, and ^{1}H–^{27}Al cross-polarization MAS NMR (CPMAS) to confirm the presence of Al[4], Al[5], and Al[6] in both precipitated C–S–H samples and white cement pastes hydrated for different lengths of time. They also examine the same samples heated to temperatures as high as 200 °C. Their results confirm the conclusion of Richardson and co-workers that Al[4] occurs on only the bridging tetrahedra of the drierkette Al-silicate chains. They propose that the Al[5] occurs in the C–S–H interlayers and that the Al[6] occurs in a hydrous aluminate or Ca-aluminate phase associated with the C–S–H particle surfaces. Based on structural–chemical considerations, they argue that the Al[6] cannot occur on the Ca-sites of the central Ca–O sheet.

Here, we use powder X-ray diffraction (XRD), compositional analysis, and ^{27}Al and ^{29}Si MAS NMR spectroscopy to investigate the structural role of Al in a series of 36 samples of semi-crystalline, precipitated, tobermorite-type C–S–H samples with varying compositions and synthesis times. The ^{27}Al NMR spectra were collected at H_0=17.5 T (corresponding ^{1}H frequency=750 MHz), providing good spectral resolution. The relatively small quadrupolar couplings observed by Faucon et al. [21–25] and Andersen et al. [30–32] suggest that the peak maxima observed at H_0=17.5T are displaced only 1–2 ppm from their isotropic chemical shifts. The spectral resolution is fully adequate to unambiguously relate the resonance to those of Faucon et al. [21–25] and Andersen et al. [30–32]. Thus, we will use these peak maxima for discussion. We have chosen to focus on just the 17.5 T ^{27}Al MAS spectra, because the isotropic chemical shifts and quadrupolar parameters of most of these sites have been previously characterized by the authors cited above, because the resolution in our MAS spectra is very good, and because MQ spectra are very time consuming to acquire, cannot be relied on to assist with determination of quantitative peak intensities, and do not provide additional structural insight [32].

2. Experimental procedure

The Al-substituted C–S–H samples were prepared by precipitation from solution at a water/solid ratio of 50. $Na_2SiO_3 \cdot 9H_2O$ (Fisher Chemicals, Certified) was dissolved in deionized water and stoichiometric amounts of $Ca(NO_3)_2 \cdot 4H_2O$ (Fisher Chemicals, Certified) and $Al(NO_3)_3 \cdot 9H_2O$ (Aldrich Chemical Company, Inc., A.C.S. reagent) were dissolved together in a separate solution. The nitrate solution was then added drop by drop into the sodium

silicate solution to give the desired starting composition. The pH of the resultant solution was adjusted to > 12 and maintained at that level by adding NaOH pellets. Maintenance of the high pH is essential to avoid the structural changes that can occur at lower values [34–37]. Precipitation occurred immediately, but the solution mixtures were allowed to react for 1 week, 4 weeks, and 4 months while being continuously rotated at 90 or 105 rpm. The solids were separated with a centrifuge and then washed with deionized water three times with centrifuging between washings. They were then washed once more with acetone and again centrifuged. The samples were then placed in an evaporating dish and kept in a box with flowing N_2 to remove acetone. After most of the solvent was removed, the samples were dried in a vacuum desiccator overnight. They were then stored in flowing N_2. All the above operations except centrifuging were carried out in a N_2 atmosphere to minimize CO_2 contamination. During centrifuging, the samples were in capped conical vials.

The initial atomic Ca/Si ratios of the starting solutions were 0.86, 1.18, and 1.40, and for each Ca/Si ratio, Al was added to replace 0, 7.5, 15, and 30 at.% of the Si. Bulk chemical analysis was done by X-ray fluorescence (XRF) at the Illinois State Geological Survey, Champaign, IL, USA. The small amount of Al_2O_3 reported for the samples with no Al input is analytical error. No ^{27}Al NMR signal could be detected for these samples. Analyses are not available for the 4-month samples, because they could not be fully dissolved in the borate flux used for XRF analysis.

Powder XRD patterns were collected on a Rigaku Geigerflex D/Max II diffractometer using the summation of, typically, four scans to improve the signal-to-noise ratio.

^{29}Si NMR spectra were recorded under MAS at 59.5 MHz (H_0 = 7.05 T) using a General Electric Model GN-300 WB spectrometer. MAS spinning frequencies were approximately 4.5 kHz. Chemical shifts were measured relative to the peak for tetra(trimethylsilyl)silane (TMSS) at −9.9 ppm. Typical ^{29}Si T_1 relaxation times measured using a standard inversion-recovery pulse sequence were approximately 70 s. Thus, about 70 transients were acquired for each spectrum using a pulse recycle delay of 350 s to ensure full relaxation.

^{27}Al NMR spectra shown were acquired under MAS conditions at 195.5 MHz using a Varian Unity 750 spectrometer (H_0 = 17.5 T). MAS spinning frequencies were 9.8 kHz. Chemical shifts are reported with respect to 1 M $[Al(H_2O)_6]^{3+}$ as an external standard. Pulse lengths were 1 μs, and recycle times 2 s, adequate for full relaxation in these hydrous samples.

3. Results and structural interpretations

3.1. Chemical compositions and XRD data

The analyzed bulk chemical compositions are in the range expected for C–S–H and show that the Ca/(Si+Al) ratios parallel the initial batched compositions but deviate progressively from them with increasing Ca content (Table 1). The analyzed Al/(Si+Al) ratios are very close to the batched compositions. The three compositional series will be referred to here by their average analyzed atomic Ca/(Si+Al) ratios of 0.86, 1.1, and 1.2. Na contents are significant, ranging from 0.49 to 6.63 at.%, and are generally largest at Ca/(Si+Al) = 0.86 and for the samples with no Al. Na content generally decreases with increasing Al/(Si+Al) at a given Ca/(Si+Al) ratio.

The XRD patterns of all the synthesized samples show typical tobermorite-type C–S–H (*I*) [7,8] with strong (hk0) peaks or (hk.) band heads at 5.3, 3.07, 2.80, 1.83, and 1.67 Å (Fig. 1) that can be readily assigned to C–S–H–I (10l), (110), (200), (020), and (310) diffractions [8]. Additional phases detected include stratlingite (C_2ASH_8), the dicalcium aluminate hexahydrate AFm phase (C_2AH_6), and the zeolite heulandite. With one exception, these additional phases occur only in the samples with the largest Al for Si replacement (30%). At Ca/(Si+Al) = 0.86, strätinglite occurs in the 4-week and 4-month samples with 30% Al for Si replacement. At Ca/(Si+Al) = 1.1, C_2AH_6 occurs in the 1-week and 4-week samples with 30% Al for Si replacement, but it disappears except for a very low peak at about 23° 2θ in the 4-month sample, paralleling the loss of AFm phases due to grinding observed by Copeland et al. [12]. At Ca/(Si+Al) = 1.2, C_2AH_6 occurs in all the samples with 30% Al for Si replacement and is joined by heulandite ($CAS_7H_{1.7}$) in the 4-month sample. C_2AH_6 also occurs in the 1-week sample with Ca/(Si+Al) = 1.2 and 15% Al substitution, but again it disappears at longer reaction times and is not present in the 4-week and 4-month samples at this composition. The C_2AH_6 probably formed by dehydration of the more hydrated AFm phase C_2AH_8 originally present in the samples [8], indicating that the samples are well dried.

The XRD data for the C–S–H of all the synthesized samples demonstrate that, as expected, it has a layered, tobermorite-like, Ca-silicate structure consisting of a central Ca–O sheet and partial or complete tetrahedral silicate chains on either side [7,8,34,37]. One of the key observations is that the positions of the (hk0) peaks do not change significantly with composition, and thus that the (200) and (020) dimensions do not deviate significantly from the ranges of 0.280 to 0.283 nm and 0.182 to 0.184 nm, respectively, observed for Al-free tobermorite-type C–S–H [34,37]. Because Si–O–T (T = Si,Al) intra-tetrahedral bond angles are relatively compliant [38], the (hk0) dimensions are controlled primarily by the central Ca–O sheet of the layer structure [7,8]. Thus, the constant (100) and (010) cell dimensions support the conclusions of Andersen et al. [30–32] that Al does not substitute significantly for Ca in the Ca–O sheet. Ca and Al have very different ionic radii (0.99 ? and 0.50 ?, respectively). As discussed by Andersen et al. [32], disordered Al for Si substitution is unlikely on structural chemical grounds. Ordered Al for Ca substitution would cause large changes in the (hk0) dimensions. For

Table 1
Compositional analyses for the C–S–H samples reacted for 1 week and 4 weeks obtained by X-ray fluorescence

Name	8-1	8-2	8-3	8-4	11-1	11-2	11-3	11-4	14-1	14-2	14-3	14-4
	Ca/(Al+Si)=0.86				Ca/(Al+Si)=1.18				Ca/(Al+Si)=1.4			
	Al/(Al+Si)				Al/(Al+Si)				Al/(Al+Si)			
	0.00	0.08	0.15	0.30	0.00	0.08	0.15	0.30	0.00	0.08	0.15	0.30
1 week oxide weight %												
SiO_2	46.12	42.41	39.51	32.96	42.09	39.65	36.37	28.64	40.96	38.07	33.06	25.60
Al_2O_3	0.94	3.63	6.39	11.17	0.75	3.29	5.87	9.88	0.50	3.24	5.34	9.39
CaO	37.39	37.05	36.87	36.27	43.55	43.97	42.79	41.33	45.69	45.08	44.65	42.71
Na_2O	3.20	2.69	2.10	1.80	1.02	0.49	0.46	0.40	0.38	0.52	1.08	0.50
Sum	87.65	85.78	84.86	82.20	87.40	87.41	85.50	80.26	87.54	86.90	84.14	78.20
1 week percentage of atoms												
Si	49.34	46.31	43.61	37.27	45.95	43.30	40.41	33.57	44.89	41.75	37.03	30.70
Al	–	4.66	8.30	14.86	0.96	4.23	7.67	13.62	0.64	4.18	7.04	13.25
Ca	42.85	43.34	43.60	43.94	50.94	51.44	50.93	51.90	53.66	52.97	53.59	54.89
Na	6.63	5.68	4.49	3.94	2.16	1.04	0.99	0.91	0.81	1.10	2.34	1.16
1 week atomic ratios												
Ca/(Si+Al)	0.85	0.85	0.84	0.84	1.09	1.08	1.06	1.10	1.18	1.15	1.22	1.25
(Ca+Na)/(Si+Al)	0.98	0.96	0.93	0.92	1.13	1.10	1.08	1.12	1.20	1.18	1.27	1.28
Al/(Al+Si)	–	0.09	0.16	0.29	0.02	0.09	0.16	0.29	0.01	0.09	0.16	0.30
4 weeks oxide weight %												
SiO_2	43.40	42.40	38.93	32.15	40.97	39.07	35.92	27.30	38.03	38.02	34.11	25.64
Al_2O_3	0.49	3.47	5.90	11.45	0.46	3.26	5.22	9.91	0.25	3.32	5.29	9.75
CaO	36.50	37.36	37.00	36.98	44.36	43.51	42.56	40.80	45.14	44.91	43.58	42.12
Na_2O	2.49	1.96	1.43	1.24	0.64	0.37	0.33	0.43	0.84	0.23	0.31	0.24
Sum	82.88	85.19	83.26	81.82	86.43	86.21	84.03	78.44	84.26	86.48	83.29	77.75
4 weeks percentage of atoms												
Si	49.37	46.95	44.10	36.68	45.38	43.30	40.68	32.66	43.06	42.02	38.93	31.00
Al	–	4.52	7.86	15.37	0.60	4.25	6.95	13.96	0.33	4.32	7.10	13.87
Ca	44.49	44.33	44.90	45.21	52.65	51.66	51.64	52.35	54.76	53.18	53.29	54.57
Na	5.48	4.20	3.14	2.74	1.37	0.79	0.72	1.00	1.84	0.49	0.68	0.56
4 weeks atomic ratios												
Ca/(Si+Al)	0.89	0.86	0.86	0.87	1.14	1.09	1.08	1.12	1.26	1.15	1.16	1.22
(Ca+Na)/(Si+Al)	1.00	0.94	0.92	0.92	1.17	1.10	1.10	1.14	1.30	1.16	1.17	1.23
Al/(Al+Si)	–	0.09	0.15	0.30	0.01	0.09	0.15	0.30	0.01	0.09	0.15	0.31

Data for the 4-month samples are not reported, because these samples could not be fully dissolved in the borate flux.

instance, the main hydroxide layer of AFm phases can be thought of as an ordered replacement of 1/3 of the Ca by Al in the Ca-hydroxide structure [8], resulting in substantial decreases of the (hk0) cell dimensions (ca. 9% in rhombohedral coordinates). Such large changes would be readily observed by XRD.

The resolution of, especially, the (200) XRD peak decreases with increasing Al-content in each series, indicating decreased in-plane order. This decreasing order suggests significant Al-incorporation in the C–S–H.

The C–S–H samples also yield strong basal (002) peaks at 2θ values less than 10° (Fig. 1; Table 2), demonstrating good layer-stacking order relative to many C–S–H samples. The basal spacings of the Al-free samples decrease with increasing Ca/Si ratio and are in the known range for dried C–S–H, varying from 12.87Å to 10.18Å. This trend has been previously observed for many C–S–H samples and is due to loss of the bridging tetrahedra in the silicate chains of the C–S–H structure [8,34,37,39]. The basal spacings increase substantially with increasing Al-content at a given Ca/(Si+Al) ratio (Fig. 1; Table 2), with values as large as 16.41Å for Al-rich samples. To our knowledge, basal spacings this large have never been observed for Al-free C–S–H or tobermorite. For a given Ca/(Si+Al) ratio and reaction time, the increase between the basal spacing of the Al-free sample and the most Al-rich one varies from 1.15Å to 3.96Å, and is greatest for the 4-month samples. These increases are much too large to be due to tetrahedral Al for Si substitution, which would have at most an effect of 0.1–0.2Å. This observation, coupled with the conclusion that the fundamental tobermorite-like Ca-silicate structure does not change, indicates that the increased basal spacings for the Al-rich samples must be due to a significant amount of Al in the interlayer. The increased basal spacings are not

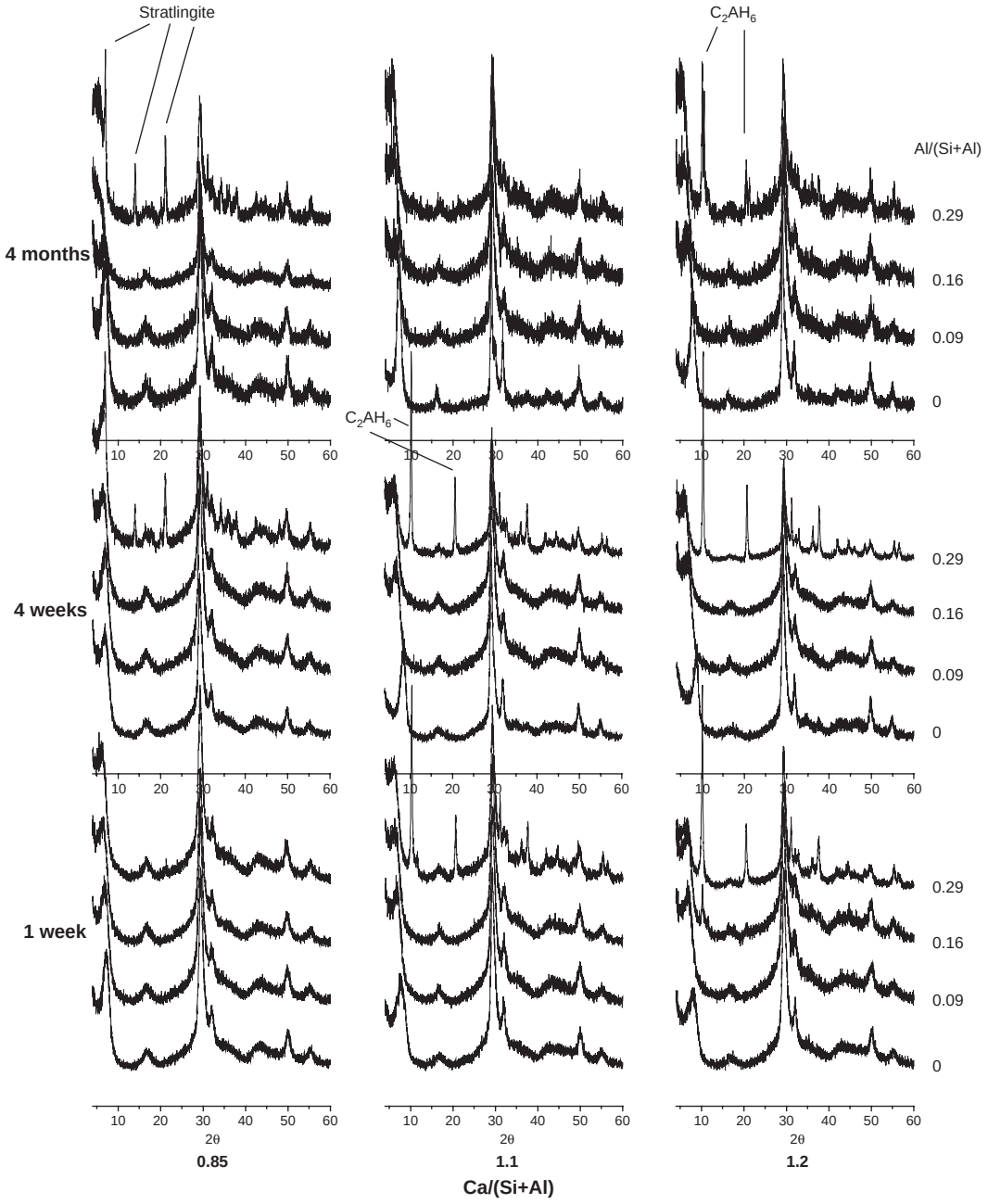

Fig. 1. Powder X-ray diffraction patterns of C–S–H samples with the indicated compositions and reacted for the indicated times.

due to increased interlayer water contents, because the XRD data were collected for well-dried samples.

3.2. ^{29}Si NMR

As in previous studies of Al incorporation into C–S–H, the ^{29}Si MAS NMR spectra clearly show significant occupancy of tetrahedral chain sites by Al, and the changes in the ^{29}Si MAS NMR spectra of our samples (Fig. 2) with changing Al-content and Ca/(Si+Al) ratio are very similar to those of previous studies [1,2,4,20–23,26,27,30–33]. The Al-free samples yield peaks for Q^1 Si-sites at about −79.7 ppm and Q^2 Si-sites at about −84.5 ppm, and the relative intensity of the Q^1 peak is much greater at Ca/(Si+Al)=1.1 and 1.2 than at 0.86. This is the trend expected with decreasing polymerization of the silicate chains, and has been observed many times. With increasing Al/(Si+Al) ratio, the relative intensity of the Q^1 peak decreases, and a peak with a maximum of about −81.5 ppm grows in intensity. Many of the spectra also contain poorly resolved intensity in the −85 to −90 ppm range that is clearly not present for the Al-free samples. Reaction time has little effect on the relative intensities. There is no ^{29}Si NMR signal for the stratlingite and

Table 2
Basal lattice spacings (Å) for the C–S–H samples in this study obtained by powder X-ray diffraction

Al/(Si+Al)	Ca/(Si+Al)=0.86				Ca/(Si+Al)=1.1				Ca/(Si+Al)=1.2			
	0	0.09	0.16	0.29	0	0.09	0.16	0.29	0	0.09	0.16	0.29
1-week	12.27	13.1	13.8	14.67	11.53	13.3	13.84	14.15	10.88	13.3	13.41	13.41
4-week	12.87	12.87	13.27	14.02	10.44	13.1	13.36	14.12	10.18	13.54	13.96	13.75
4-month	12.65	13.08	–	16.41	12.07	13.8	14.17	15.28	11.21	13.54	14.29	15.17

heulandite above the noise level. The peak for a small amount of stratlingite at −86.7 ppm [40,41] would be lost in the main C–S–H peaks.

For both tobermorite and C–S–H, the peak at about −81.5 ppm has been well assigned to Si on Q^2 sites with 1 tetrahedral Si next-nearest neighbor (NNN) and 1 tetrahedral Al NNN (Q^2[1Al] sites). Its increase in intensity with increasing Al/(Si+Al) ratio and the simultaneous loss of intensity for the Q^1 peak indicate that Al enters the tetrahedral chain sites and that the alumino-silicate chains become progressively more polymerized with increasing Al/(Si+Al), as suggested by previous workers [1,26,30,32]. The tobermorite structures contain 3-repeat tetrahedral chains (drierkette) in which the two non-bridging oxygen atoms of pairing tetrahedra are part of the central Ca–O sheet [8,39,53]. In contrast, the bridging tetrahedra expose their two non-bridging oxygens to the interlayer, in which they play a range of structural roles including cross-linking across the interlayer. In tobermorite-like C–S–H, decreasing occupancy of the bridging tetrahedral sites leads to increasing Ca/Si ratios and increasing intensity of the Q^1 ^{29}Si resonance. Increasing occupancy of bridging tetrahedral sites by Al[4] decreases the Ca/(Si+Al[4]) ratio, connects chain segments, changes Q^1 Si-sites to Q^2 (1Al) sites, and increases the average polymerization of the tetrahedral chains [1,26,30,32]. Many tobermorites and low Ca/Si tobermorite-like C–S–Hs also contain Q^3 sites due to cross-linking of bridging tetrahedra across the interlayer. In Al-free tobermorites, these resonate near −96 ppm [12,13,15], and in Al-free C–S–H, they result in a band of intensity from about −89 to −97 [34,37]. In cross-linked tobermorites, Al[4] for Si substitution causing Al[4]–O–Si linkages results in ^{29}Si NMR signal for Q^3(1Al) sites between about −91 and −94 ppm [12,13,15]. Our spectra contain significant intensity in this range, indicating the occurrence of comparable sites.

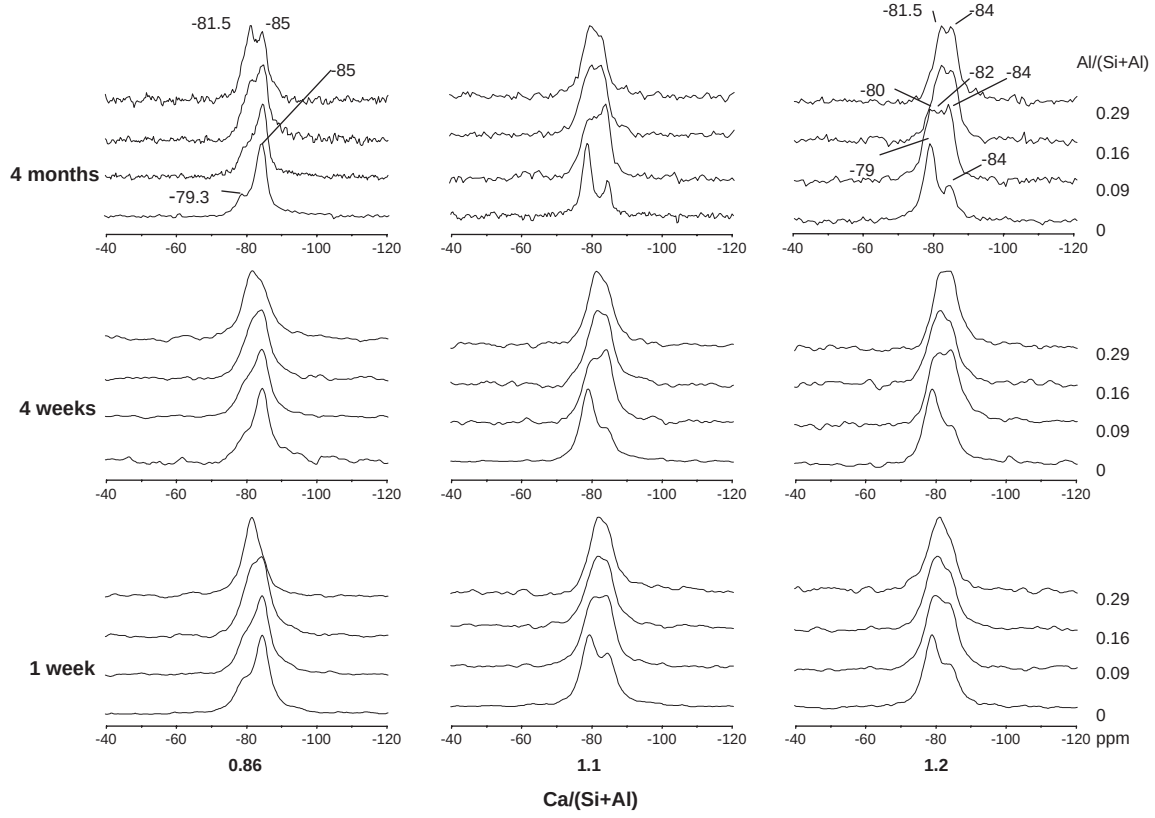

Fig. 2. ^{29}Si MAS NMR spectra of C–S–H samples with the indicated compositions and reacted for the indicated times.

As discussed above, there has been considerable controversy in the literature about whether Al[4] occupies only the bridging tetrahedral sites or also the pairing sites. The absence of ^{29}Si NMR signal in the −75 to −80 ppm range that would suggest significant concentrations of Q^1[1Al] Si-sites that are chain-ending or in dimers supports the conclusions of Richardson and co-workers [1,26–28] and Andersen et al. [30–32] based on TMS and NMR data that Al does not significantly occupy the pairing tetrahedra. Structurally, it is more likely that Al will enter the bridging tetrahedra, because Al[4]–O bonds are typically about 0.1 Å longer than Si–O bonds, and the larger Al–O tetrahedra have more room to fit into the structure at the bridging sites. This is because the positions of the two non-bridging oxygens pointing into the interlayer are less constrained than those of the non-bridging oxygens of the pairing tetrahedra, which are coordinated to the Ca's of the structurally constrained central Ca-layer [8]. The reduced constraint on the bridging tetrahedra is probably the reason that Al[4] occurs in tobermorites and C–S–H, but not in denser chain silicates with drierkette tetrahedral chains, such as wollastonite, in which the bridging tetrahedra are coordinated to Ca's with well-defined structural positions. Al[4] for Si substitution also requires additional positive charge for local and overall charge balance, and in C–S–H, it is more difficult to charge balance Al[4] on the pairing sites than on the bridging sites. The only location for additional positive charge on next-nearest neighbor positions to Al[4] on the pairing tetrahedra is in the main layer. Al^{+3} for Ca^{+2} substitution there would provide this charge, but is ruled out by the XRD data and the structural chemical considerations of Andersen et al. [30–32]. In contrast, the non-bridging oxygens of the bridging tetrahedra, that are surface sites or on the walls of the interlayer space, can be coordinated to additional charge balancing alkali cations, Ca^{+2}, Al^{+3}, or H^+(to form OH-groups) [20].

3.3. ^{27}Al NMR

The ^{27}Al NMR spectra of our samples show signal that is readily assignable to Al[4], Al[5], and Al[6] with peak maxima near, respectively, 58 to 74 ppm, 35 ppm, and 4 ppm [4,12–19,30–32,42–48] (Fig. 3). Those samples that contain stratlingite or C_2AH_6 as detected by XRD also yield ^{27}Al signal assignable to that phase. The stratlingite yields narrow peaks for Al[4] at 62 ppm and Al[6] at 10 ppm [40,41], and the C_2AH_6 yields the narrow Al[6] peak near 10 ppm [19,30–32,45,46]. The heulandite ($CAS_7H_{1.7}$) may cause the Al[4] peak near 63 ppm for the high Al-content 4-month samples at Ca/(Si+Al)=1.1 and 1.2, although a minor amount of Si in the AFm phase (stratlingite solid solution) may also cause this signal.

Because there is no chemical, XRD, or ^{29}Si NMR evidence for phases other than tobermorite-type C–S–H, stratlingite, C_2AH_6, and heulandite, it is likely that all the other Al[4], Al[5], and Al[6] resonances are due to Al associated with the C–S–H. Indeed, all of them have been previously observed for C–S–H or tobermorite. For our C–S–H, there is one Al[6] peak with a maximum at 4 ppm, one Al[5] peak with a maximum at 36 ppm, and three Al[4] peaks or shoulders with maxima at 58, 66, and 74 ppm. Although there are clear changes in the relative intensities of these resonances, the positions of the peak maxima do not vary, indicating that the local structural environments of the Al causing these resonances are similar in all the samples. The 4 ppm peak is well resolved from the Al[6] resonances for C_2AH_6 and stratinglite. It corresponds to the Al[6] resonances observed for precipitated C–S–H by Faucon et al. [25] (isotropic chemical shift (δ_i)=~4.5 ppm) and for hydrated white cement pastes and precipitated C–S–H by Andersen et al. [30–32] (δ_i=~5.0 ppm). The 36 ppm peak corresponds to the Al[5] resonances of C–S–H observed for precipitated C–S–H by Faucon et al. [25] (δ_i=~38.5 ppm) and for hydrated white cement pastes and synthetic C–S–H by Andersen et al. [30–32] (δ_i=~39.9 ppm). These Al[6] and Al[5] peaks are not observed for aluminous tobermorites [12,13,15]. The 58, 66, and 74 ppm resonances for our samples correspond to Al[4] resonances observed by Faucon et al. [25] with the following parameters: δ_i about 58–60 ppm and ν_Q about 0.33, δ_i about 67 ppm and ν_Q about 0.46, and δ_i about 75 ppm and ν_Q about 0.45. ν_Q is the quadrupolar frequency, which has units of MHz and is related to the quadrupole coupling constant (C_Q), quadrupole asymmetry parameter (η), and nuclear spin (I) as described in Ref. [23]. The 58 and 66 ppm resonances are also observed for tobermorites, but the 74 ppm resonance is not [12,13,15]. The peak maxima reported for the tobermorites occur at slightly less positive peak maxima than the isotropic chemical shifts, due to the relatively low H_0 field available for the tobermorite studies. The 14.1 T ^{27}Al NMR spectra for hydrated white cement pastes shown by Andersen et al. [30–32] do not contain resolvable multiple Al[4] resonances, but their spectra for synthetic C–S–Hs clearly show an Al[4] resonance with a center of gravity near 75 ppm that dominates at Ca/Si ratios ≥ 1.25 and a second one centered near 66 ppm that is prominent at Ca/Si ratio of 0.75 and 0.83. In addition, their Ca/Si=0.66 sample yields a broad Al[4] resonance centered near 61 ppm. Faucon et al. [25] grouped the 58 and 66 ppm resonances together, but our spectra and the data for tobermorites clearly show that they are different.

Because of peak overlap and likely asymmetrical peak shapes [21–25,30–32], we have chosen not to curve fit individually the intensities of the three Al[4] peaks in our spectra, but the following points are clear. The 58 ppm resonance is present for many samples and is most intense for those with the smallest Ca/(Si+Al) ratios and the least Al[5]+Al[6] intensity. The 66 ppm resonance is present as a peak or shoulder for all the samples and has the highest peak maximum for many of them. The 74 ppm resonance is also present for all the samples and is most intense for those with relatively large Al[5]+Al[6] intensities.

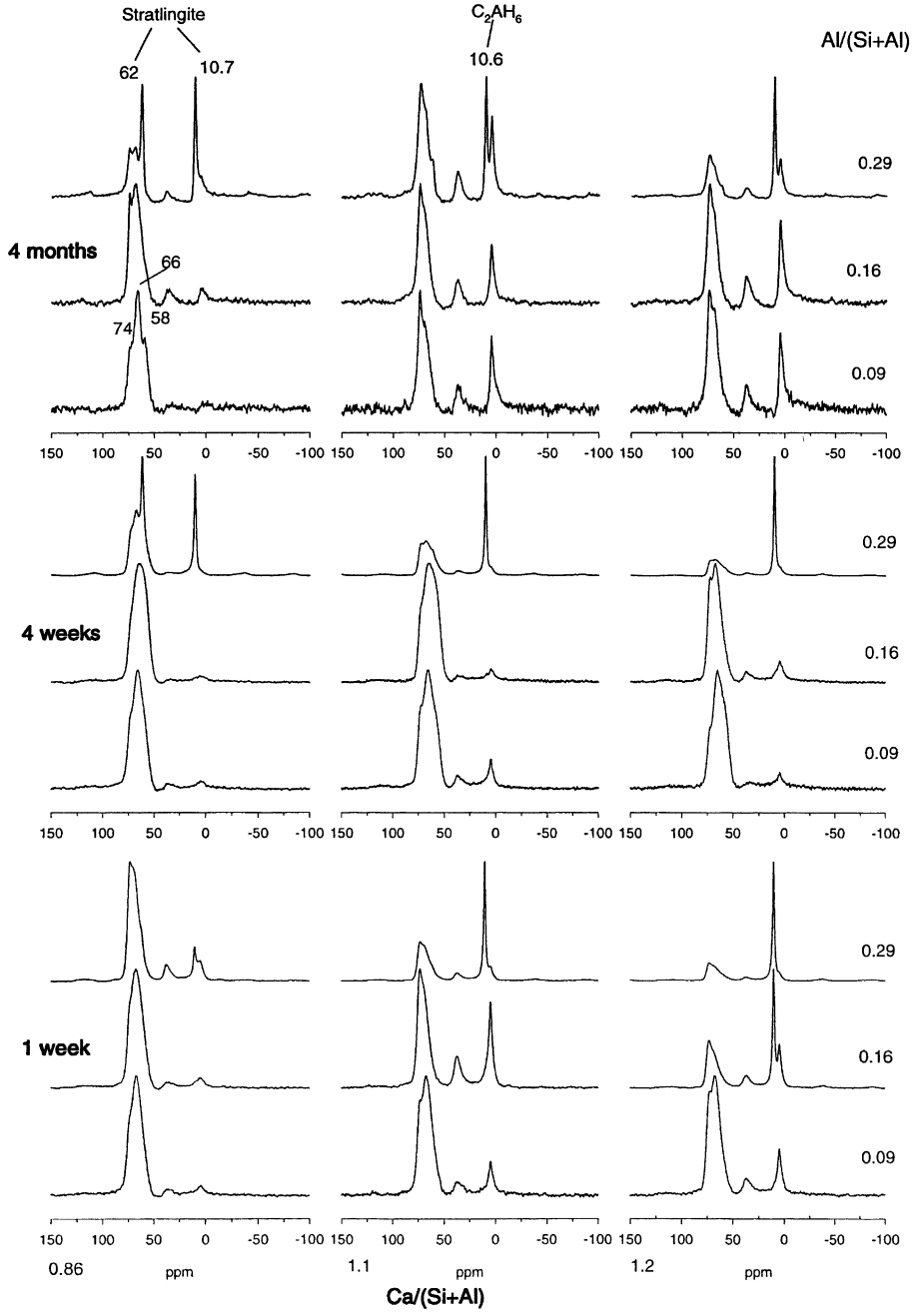

Fig. 3. ^{27}Al MAS NMR spectra of C–S–H samples with the indicated compositions and reacted for the indicated times. The spectra were obtained at $H_0 = 17.5$ T.

As previously observed by Stade and Müller [16] and Richardson et al. [1,26,27], the Al[4]/(Al total) ratios for our samples decrease with increasing Ca/(Si+Al) ratio (Fig. 4). The quantitative analyses of Andersen et al. [30–32] suggest that quadrupolar effects probably do not significantly influence the observed relative ^{27}Al NMR peak intensities for the different sites at the high field used here. For our samples, the Al[4]/(Al Total) ratios are quite variable for the 1-week samples (especially at Ca/(Si+Al)s = 1.1 and 1.2), suggesting that the initial, rapid precipitation leads to a wide variety of local structures. At 4 weeks, Al[4]/(Al Total) ratios are generally larger and become less scattered, and at 4 months, they again decrease. These observations, together with the observed loss of C_2AH_6 with increasing reaction time and the generally increasing XRD basal spacings especially at large Al-contents discussed above, demonstrate that the rapidly precipitated, initial C–S–H continues to react over periods of weeks to months and that the Al-environments associated with the C–S–H are chemically quite labile during this time. The insolubility of the 4-month samples in the borate flux used for XRF chemical analysis indicates the formation of a chemically quite recalcitrant and probably more stable material containing

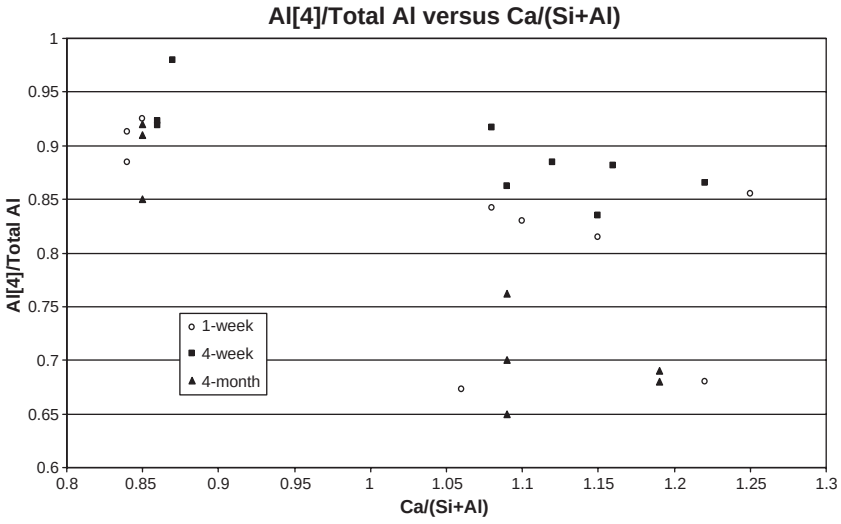

Fig. 4. Al[4]/(Al Total) in C–S–H obtained by curve fitting of the observed ^{27}Al MAS NMR spectra plotted versus analyzed Ca/(Si+Al) atomic ratio. NMR signal for secondary phases is not included.

relatively more Al[5] and Al[6] than the early-formed material.

4. Structural model

The compositional, XRD and NMR data presented here together with the published NMR and TMS data for C–S–H and NMR data for tobermorites discussed above support a structural model for Al incorporation into tobermorite type C–S–H the involves Al[4] occupancy of three types of bridging tetrahedral sites and Al[5] and Al[6] occupancy of interlayer sites. Andersen et al. [30–32] have suggested that the Al[5] occurs in the interlayers and that the Al[6] occurs on the surfaces of C–S–H particles. Our results do not preclude surface precipitates, and because the silicate sites exposed on C–S–H surfaces are likely to be similar to those on the walls of the interlayer, such surface precipitates are likely to be present. Key points in support of our conclusions are the following. (1) The XRD data show no significant change in the (hk0) dimensions of our samples with Al content, precluding significant Al occupancy of the central Ca–O sheet and supporting the structural chemical arguments of Andersen et al. [30–32]. (2) The XRD data do show large increases in the (002) basal spacing with increasing Al-content, with spacings as large as 16.4 Å. These spacings are strong evidence for incorporation of significant amounts of Al in the interlayers of at least these preparations. (3) In tobermorite type C–S–H, tetrahedral chain sites are available for occupancy by Al[4], and all available ^{29}Si NMR and TMS data support Al occupancy of principally the bridging tetrahedra. (4) There are three Al[4] sites in aluminous C–S–H, two of which are present for aluminous tobermorites. (5) Aluminous tobermorites do not contain Al[5] or Al[6], and the Al[4] resonance at 74 ppm that is not present for tobermorites increases in intensity with increasing Al[5]+Al[6] content of the C–S–H.

Assignment of the three Al[4] resonances can be confidently made based on the spectra presented here, the known structural chemical controls on ^{27}Al chemical shifts [17–19,42–50], and the results for aluminous tobermorites of Komernani and coworkers [12,13,15]. From the literature, it is well known that ^{27}Al NMR chemical shifts have more positive values with decreasing polymerization and increasing linkage to other Al-sites (see Ref. [48] for a comprehensive compilation of NMR chemical shifts). For aluminous tobermorites, Komernani et al. [12,13,15] have reported Al[4] on both chain (Q^2) and branching (Q^3) sites, and the well known effects of polymerization on ^{27}Al chemical shifts lead to assignment of the peak near 66 ppm to Q^2 sites and the peak near 58 ppm to Q^3 sites. Structurally, the Q^3 sites link tetrahedra across the interlayer. We make these two assignments for tobermorite-type C–S–H because of their clear connections to the known structures of tobermorites, the known structural controls on ^{27}Al chemical shifts, and the dominance of the 58 ppm peak for our samples with the lowest Ca/(Si+Al) ratios, which are expected to have the highest concentration of Q^3 sites [1,34–37,39,53,54]. We assign the ^{27}Al[4] resonance with a peak maximum of 74 ppm to Al on bridging tetrahedra that is charge balanced by interlayer or surface Al[5] and Al[6] and linked to them through Al–O–Al bonds. Formation of Al[4]–O–Al[5,6]–O–Al[4] linkages across the interlayer would add as much as 3–4Å to the basal spacing, depending on the local structural configuration, in good agreement with the maximum observed change basal spacings as large as 16.4Å. This increase is non-collapsible on drying, in contrast to what would happen if the expansion was due to additional interlayer water molecules. The more positive chemical shift of 74 ppm is also consistent with this assignment. Most Al[4] in Ca-aluminates with Al–O–Al linkages has chemical

shifts between 75 and 86 ppm, and Al[4] on Q^2 sites in K and Ba aluminates with Al–O–Al linkages has chemical shifts between 80 and 83 ppm [48]. Linkage to neighboring Si-tetrahedra would cause increased shielding (less positive chemical shifts) into the range observed for the C–S–Hs [48]. Faucon et al. [25] have assigned the ^{27}Al resonances with isotropic chemical shifts from ca. 58 to 67 ppm to Al[4] on the pairing tetrahedra (non-bridging tetrahedra in their nomenclature) and the resonances with isotropic chemical shifts of ca. 74–75 ppm to Al[4] on the bridging tetrahedra. These assignments fail to take into account the presence of three resolvable Al[4] resonances and the results for the aluminous tobermorites. They are unlikely to be correct for the reasons described above.

In tobermorite-like models of C–S–H, all Al[4] must be charge balanced with an additional net+1 charge, because of the difference in charge between Al^{+3} and $Si.^{+4}$ The Al on the bridging tetrahedral sites responsible for the 58 ppm (Q^3) and 66 ppm (Q^2) peaks could be charge balanced by interlayer (or surface) Na^+, Ca^{+2}, or H^+ (OH-groups). All our samples have significant levels of Na that cannot be removed by washing in water, indicating that Na plays an important charge balancing role for our samples, as suggested by previous workers [20–25]. Preliminary ^{23}Na MAS NMR spectra for some of our samples show that Na occurs on sites that allow it to become mobile (solution-like) when the sample is wet (probably surface sites) and also on sites that are rigidly held in the structure (probably interlayer sites; data not shown). Charge balancing of Al[4] (here the 74 ppm peak) by Al[5] and Al[6] is well known in many compounds, including a wide range of Al-silicates (sillimanite, Al-rich pyroxenes) and is also consistent with the structures of amorphous alumina and silico-aluminate phases and many Al-rich glasses [47–52]. Al[5] is well known to occur in many of the amorphous phases. Bunker et al. [51] describe many potentially stable nearest neighbor and next-nearest neighbor structural configurations involving Al[4], Al[5], and Al[6]. The ^{1}H–^{27}Al CPMAS NMR data of Andersen et al. [32] demonstrate that H is likely to occur in the next-nearest neighbor structural environment of the Al[6] associated with C–S–H, and their data also show that these Al[6] structural environments begin to decompose to Al[4] and Al[5] at temperatures as low as 70 °C. These observations clearly demonstrate that the Al[6] associated with C–S–H occurs in hydrous environments involving H_2O or OH-groups coordinated to the Al. The Al[5] and Al[6] environments may also involve additional charge balancing species such as Na^+ and Ca^{+2}, and Bunker et al. [51] describe many possible nearest- and next-nearest-neighbor configurations.

The results described here, the recent results of Andersen et al. [30–32], and the previous results for aluminous tobermorites and C–S–H discussed above lead to an overall model for incorporation of Al in tobermorite-type C–S–H with the following features. (1) The structural core of the tobermorite-type layers, consisting of the central Ca–O sheet and the pairing tetrahedra, is essentially unmodified by Al incorporation. (2) Al[4] occurs on the bridging tetrahedra of the drierkette chains with both Q^2 and Q^3 linkages, and is charge balanced by alkali cations, Al[5] and Al[6], and possibly Ca^{+2} and H^+. (3) The Al[5] and Al[6] occur in hydrous aluminate, Ca-aluminate, or Na-aluminate environments associated with C–S–H in the interlayer galleries and/or on particle surfaces.

For our samples, the Al occurs primarily as Al[4] on Q^2 and Q^3 sites at relatively low Ca/(Si+Al) ratios in the range of crystalline tobermorites (here 0.86), and there is a small amount of Al[5] and Al[6]. The Al[4] is charged balanced by interlayer and surface Na^+, possibly by Ca^{+2} and OH^-, and to some extent by interlayer or surface Al[5] and Al[6]. At higher Ca/(Si+Al) ratios (here 1.1 and 1.2), Al[4] occurs primarily on Q^2 bridging sites and a greater fraction of the total Al occurs as Al[5] and Al[6]. Thus, more of the Al[4] is charged balanced by interlayer and surface Al[5] and Al[6]. The polymerization of the alumino-silicate drierkette chains increases with increasing Al/(Si+Al) ratio as Al enters the bridging tetrahedral sites and links portions of alumino-silicate chains that are disconnected at lower Al-contents.

The compositional data in Table 1 together with curve fitting of our ^{27}Al MAS NMR spectra (data in Fig. 4) show that the maximum total Al/(Si+Al) ratio in the C–S–H of our samples is about 23%, and typical values are about 21%. Based on these values and the Al[4]/(Al Total) ratios in Fig. 4, the maximum substitution of Al[4] for Si[4] in the chains (Al[4]/Si+Al[4]) is about 0.22. This value is slightly lower than the value of 0.26 determined by Faucon et al. [22], but the estimates are in reasonably good agreement. The comparable Al[4]/(Si+Al[4]) ratios for the 4-month samples, that may be closer to equilibrium than those reacted for shorter times, are about 0.17, reflecting increased relative abundances of Al[5] and Al[6]. This value is approximately 1/6 of all tetrahedra, or 1/2 of the bridging tetrahedra for a fully polymerized structure.

The substantial remaining challenge concerning aluminous C–S–H is to better define the compositions and structures of the interlayer and surface environments that involve Al[5] and Al[6]. The presence of these environments is likely to lead to quite different chemical behavior than for Al-free C–S–H. The alteration of the ion exchange properties of tobermorite by Al-substitution [14,15], the effects of Al on the chemical behavior of modified cements for waste applications [5,6], the low temperatures of thermal breakdown of the Al[6] environments [32], and increased chemical durability such as the insolubility of our 4-month samples in the borate XRF flux illustrate only a few of the properties that may be affected by Al-incorporation in C–S–H. Unfortunately, definitive understanding of the local and extended structures involved is likely to be quite difficult. It appears that the Al[5] and Al[6] environments do not occur in tobermorites, and they will thus be difficult to investigate by diffraction methods. Additional spectroscopic methods, such as the NMR

dipolar recoupling technique known as REDOR and computational molecular modeling approaches may prove to be useful. Understanding the similarities and differences in the structural and chemical roles of Al in precipitated C–S–H and in the C–S–H of hydrated cement paste and the time evolution of these roles is also a central issue.

Acknowledgements

This research was supported by the NSF Center for Advanced Cement-Based Materials (ACBM). We are pleased to acknowledge useful discussions with Prof. H. F. W. Taylor, Dr. Ian G. Richardson, Dr. Adrian Brough, Dr. Jørgen Skibsted, and Dr. Morten D. Andersen concerning the role on Al in C–S–H.

References

[1] I.G. Richardson, The nature of C–S–H in hardened cements, Cem. Concr. Res. 29 (1999) 1131–1147.
[2] I.G. Richardson, J.G. Cabrera, The nature of C–S–H in model slag-cements, Cem. Concr. Res. 22 (2000) 259–266.
[3] A.R. Brough, A. Katz, G.-K. Sun, L.J. Struble, R.J. Kirkpatrick, J.F. Young, Adiabatically cured alkali-activated cement-based wasteforms containing high levels of fly ash, formation of zeolites and Al-substituted C–S–H, Cem. Concr. Res. 31 (2001) 1437–1447.
[4] J. Schneider, M.A. Cincotto, H. Panepucci, ^{29}Si and ^{27}Al high-resolution NMR characterization of calcium silicate hydrate phases in activated blast-furnace slag pastes, Cem. Concr. Res. 31 (2001) 993–1001.
[5] O.P. Shrivastava, R. Shrivastava, Sr^{+2} uptake and leachability study on cured aluminum-substituted tobermorite-OPC admixtures, Cem. Concr. Res. 31 (2001) 1251–1225.
[6] S.Y. Hong, F.P. Glasser, Alkali adsorption by C–S–H and C–A–S–H gels: Pt. II. Role of alumina, Cem. Concr. Res. 32 (2002) 1101–1111.
[7] H.F.W. Taylor, Nanostructure of C–S–H: current status, Adv. Cem. Based Mater. 1 (1993) 38–46.
[8] H.F.W. Taylor, Cement Chemistry, 2nd ed., Thomas Telford Publishing, London, 1997.
[9] H.M. Jennings, Colloid model of C–S–H and implication to the problems of creep and shrinkage, Mat. Struct. 37 (2004) 59–70.
[10] G.L. Kalousek, Crystal chemistry of hydrous calcium silicates: I. Substitution of aluminum in lattice of tobermorite, J. Am. Ceram. Soc. 40 (1957) 74–80.
[11] L.E. Copeland, E. Bodor, T.N. Chang, C.H. Weise, Reactions of tobermorite gel with aluminates, ferrites, and sulfates, J. Res. Dev. Lab., Portland Cem. Assoc. 9 (1967) 61–74.
[12] S. Komarneni, R. Roy, D. Roy, C. Fyfe, G. Kennedy, A. Bothner-By, J. Dadok, A. Chesnick, ^{27}Al and ^{29}Si magic angle spinning nuclear magnetic resonance spectroscopy of Al-substituted tobermorites, J. Mater. Sci. 20 (1985) 4209–4214.
[13] S. Komarneni, D.M. Roy, C.A. Fyfe, G.J. Kennedy, Naturally occurring 1.4 nm tobermorite and synthetic jennite: characterization by ^{27}Al and ^{29}Si MASNMR spectroscopy and cation exchange properties, Cem. Concr. Res. 17 (1987) 891–895.
[14] S. Komarneni, M. Tsuji, Selective cation exchange in substituted tobermorite, J. Am. Ceram. Soc. 72 (1989) 1668–1674.
[15] M. Tsuji, S. Komarneni, P. Malla, Substituted tobermorites: ^{27}Al and ^{29}Si MAS NMR, cation exchange, and water sorption studies, J. Am. Ceram. Soc. 74 (1991) 274–279.
[16] H. Stade, D. Müller, On the coordination of Al in ill-crystallized C–S–H phases formed by hydration of tricalcium silicate and by precipitation reactions at ambient temperature, Cem. Concr. Res. 17 (1987) 553–561.
[17] R.J. Kirkpatrick, X.D. Cong, An introduction to ^{27}Al and ^{29}Si NMR spectroscopy of cements and concretes, in: P. Colombet, A.R. Grimmer (Eds.), Application of NMR Spectroscopy to Cement Science, Gordon and Breach, Amsterdam, 1994, pp. 55–77.
[18] J. Skibsted, H.J. Jakobsen, C. Hall, Direct observation of aluminum guest ions in the silicate phases of cement minerals by ^{27}Al MAS NMR spectroscopy, J. Chem. Soc., Faraday Trans. 90 (1994) 2095–2098.
[19] J. Skibsted, J. Jakobsen, Characterization of the calcium silicate and aluminate phases in anhydrous and hydrated portland cements by ^{27}Al and ^{29}Si MAS NMR spectroscopy, in: P. Colombet, A.R. Grimmer, H. Zanni, P. Sozzani (Eds.), Nuclear Magnetic Resonance Spectroscopy of Cement Based Materials, Springer-Verlag, Berlin, 1998.
[20] I. Lognot, I. Klur, A. Nonat, NMR and infrared spectroscopies of C–S–H and Al substituted C–S–H synthesized in alkaline solution, in: P. Colombet, A.R. Grimmer, H. Zanni, P. Sozzani (Eds.), Nuclear Magnetic Resonance Spectroscopy of Cement Based Materials, Springer-Verlag, Berlin, 1998.
[21] P. Faucon, J.F. Jacquinot, F. Adenot, N. Gautier, D. Massiot, J. Virlet, ^{27}Al MAS NMR study on cement paste degradation by water, in: P. Colombet, A.R. Grimmer, H. Zanni, P. Sozzani (Eds.), Nuclear Magnetic Resonance Spectroscopy of Cement Based Materials, Springer-Verlag, Berlin, 1998.
[22] P. Faucon, T. Carpentier, A. Nonat, J.C. Petit, Triple-quantum two-dimensional ^{27}Al magic angle nuclear magnetic resonance study of the aluminum incorporation in calcium silicate hydrates, J. Am. Chem. Soc. 120 (1998) 12075–12082.
[23] P. Faucon, T. Carpentier, D. Bertrandie, A. Nonat, J. Verlet, J.C. Petit, Characterization of calcium aluminate hydrates and related hydrates of cement pastes by ^{27}Al MQ-MAS NMR, Inorg. Chem. 37 (1998) 3726–3733.
[24] P. Faucon, J.C. Petit, T. Carpentier, J.F. Jacquinot, F.J. Adenot, Silicon substitution for aluminum in calcium silicate hydrates, J. Am. Ceram. Soc. 82 (1999) 1307–1312.
[25] P. Faucon, A. Delagrave, J.C. Petit, C. Richet, J.M. Marchand, H. Zanni, Aluminum incorporation in calcium silicate hydrates (C–S–H) depending on their Ca/Si ratio, J. Phys. Chem., B 103 (1999) 7796–7802.
[26] I.G. Richardson, G.W. Groves, The Incorporation of minor and trace elements into calcium silicate hydrate (C–S–H) gel in hardened cement pastes, Cem. Concr. Res. 23 (1993) 131–138.
[27] I.G. Richardson, A.R. Brough, R. Brydson, G.W. Groves, C.M. Dobson, Location of aluminum in substituted calcium silicate hydrate (C–S–H) gels as determined by ^{29}Si and ^{27}Al NMR and EELS, J. Am. Ceram. Soc. 76 (1993) 2285–2288.
[28] B. Brydson, I.G. Richardson, D.W. McComb, G.W. Groves, Parallel electron energy loss spectroscopy study of Al-substituted calcium silicate hydrate (C–S–H) phases present in hardened cement pastes, Solid State Commun. 88 (1993) 183–187.
[29] C.A. Love, I.G. Richardson, The composition and structure of C–S–H in blended cement pastes containing fly ash, Inst. Phys. Conf. Ser. 161 (1999) 393–396.
[30] M.D. Andersen, H.J. Jakobsen, J. Skibsted, Incorporation of aluminum in the calcium silicate hydrate (C–S–H) of hydrated Portland cements: a high-field ^{27}Al and ^{29}Si MAS NMR investigation, Inorg. Chem. 42 (2003) 2280–2287.
[31] M.D. Andersen, H.J. Jakobsen, J. Skibsted, Characterization of white Portland cement hydration and the C–S–H structure in the presence of sodium aliminate by ^{27}Al and ^{29}Si MAS NMR spectroscopy, Cem. Concr. Res. 43 (2004) 857–868.
[32] M.D. Andersen, H.J. Jakobsen, J. Skibsted, A new aluminum-hydrate phase in hydrated Portland cements characterized by ^{27}Al and ^{29}Si MAS NMR spectroscopy, Cem. Concr. Res. 36 (2005) 3–17.

[33] S. Kwan, J. LaRosa-Thompson, M. Grutzeck, Structures and phase relations of aluminum-substituted calcium silicate hydrate, J. Am. Ceram. Soc. 79 (1996) 967–971.
[34] X.-D. Cong, R.J. Kirkpatrick, ^{29}Si MAS NMR study of the structure of calcium silicate hydrate, Adv. Cem. Based Mater. 3 (1996) 144–156.
[35] X.-D. Cong, R.J. Kirkpatrick, J.L. Yarger, P.F. McMillan, The structure of calcium silicate hydrate: NMR and Raman spectroscopic results, in: P. Colombet, A.R. Grimmer, H. Zanni, P. Sozzani (Eds.), Nuclear Magnetic Resonance Spectroscopy of Cement Based Materials, Springer-Verlag, Berlin, 1998.
[36] P. Yu, R.J. Kirkpatrick, B. Poe, P.F. McMillan, X.-D. Cong, The structure of calcium silicate hydrate (C–S–H): near-, mid-, and far-infrared spectroscopy, J. Am. Ceram. Soc. 82 (1999) 742–748.
[37] X.-D. Cong, ^{29}Si and ^{17}O nuclear magnetic resonance investigation of the structure of calcium silicate hydrate, PhD Thesis, University of Illinois at Urbana-Champaign, 1994, 171 pp.
[38] G.V. Gibbs, M.B. Boisen, L.L. Beverly, K.M. Rosso, A computational quantum chemical study of the bonded interactions in earth materials and structurally and chemically related molecules, in: R.T. Cygan, J.D. Kubicki (Eds.), Molecular Modeling Theory and Applications in the Geosciences, Mineralogical Society of America, Washington, D.C., 2001.
[39] S.A Hamid, The structure of the 11 Å tobermorite $Ca_{2.25}\{Si_3O_{7.5}](OH)_{1.5}.1H_2O$, Z. Kristallogr. 154 (1981) 189–198.
[40] R. Rinaldi, M. Sacerdoti, E. Passaglia, Stratlingite: crystal structure, chemistry, and a reexamination of its polytype vertumnite, Eur. J. Mineral. 2 (1990) 841–849.
[41] S. Kwam, J. LaRosa, M.W. Grutzeck, ^{29}Si and ^{27}Al MASNMR study of stratlingite, J. Am. Ceram. Soc. 78 (1995) 1921–1926.
[42] D. Müller, D. Hoebbel, W. Gessner, ^{27}Al NMR studies of aluminosilicate solutions. influences of the second coordination sphere on the shielding of aluminum, Chem. Phys. Lett. 84 (1981) 25–29.
[43] D. Müller, W. Gessner, Determination of the aluminum coordination in aluminum–oxygen compounds by solid-state high-resolution ^{27}Al NMR, Chem. Phys. Lett. 79 (1981) 59–62.
[44] D. Müller, A. Rettel, W. Gessner, J.P. Bayoux, A. Capmas, Progress in the ^{27}Al MAS NMR spectroscopy monitoring the hydration of calcium aluminate cements, Proc. 9th Intern. Congr. Chem. Cem., New Delhi, vol. VI, 1992, pp. 148–154.
[45] J. Skibsted, E. Henderson, H.J. Jakobsen, Characterization of calcium aluminate phases in cements by ^{27}Al MAS NMR spectroscopy, Inorg. Chem. 32 (1993) 1013–1027.
[46] X. Cong, R.J. Kirkpatrick, Hydration of calcium aluminate cements: a solid state ^{27}Al NMR study, J. Am. Ceram. Soc. 76 (1993) 409–416.
[47] M. Toba, F. Mizukami, S. Niwa, T. Sano, K. Maeda, H. Shoji, Effect of preparation methods on properties of amorphous alumina/silicas, J. Mater. Chem. 4 (1994) 1131–1135.
[48] J.F. Stebbins, Nuclear magnetic resonance spectroscopy of silicates and oxides in geochemistry and geophysics, T.J. Ahrens (Ed.), Mineral Physics and Crystallography, a Handbook of Physical Constants, vol. 2, American Geophysical Union, Washington, DC, 1995.
[49] T. Luong, H. Mayer, H. Eckert, T.I. Novinson, In situ ^{27}Al NMR studies of cement hydration: the effect of Li containing accelerators, J. Am. Ceram. Soc. 72 (1989) 2136–2141.
[50] K.J.D. Mackenzie, J.S. Hartman, K. Okada, Evidence for the presence of silicon in the alumina spinel from thermally transformed kaolinite, J. Am. Ceram. Soc. 79 (1996) 2980–2982.
[51] B.C. Bunker, R.J. Kirkpatrick, R. Brow, G.L. Turner, C. Nelson, Locals structure of alkaline-earth boroaluminate crystals and glasses: II. ^{11}B and ^{27}Al MAS NMR spectroscopy of alkaline-earth boroaluminate glasses, J. Am. Ceram. Soc. 74 (1991) 1430–1438.
[52] R.J. Kirkpatrick, R.K. Brow, NMR investigations of phosphate containing glasses, Solid State Nucl. Magn. Reson. 5 (1995) 9–15.
[53] S. Merlino, E. Bonaccorsi, T. Armbruster, The real structure of tobermorite 11 Å: normal and anomalous forms, OD character and polytypic modifications, Eur. J. Mineral. 13 (2000) 557–590.
[54] E. Bonaccorsi, S. Merlino, H.F.W. Taylor, The crystal structure of jennite, $Ca_9Si_6O_{18}(OH)_6{\cdot}8H_2O$, Cem. Concr. Res. 34 (2004) 1481–1448.